Biophysical Journal, Volume 99

Supporting Material

On the question of hydronium binding to ATP-synthase membrane rotors

Vanessa Leone, Alexander Krah, and Jose D Faraldo-Gomez

On the question of hydronium binding to ATP-synthase membrane rotors

SUPPLEMENTARY MATERIAL

Vanessa Leone,*‡ Alexander Krah,*‡
and José D. Faraldo-Gómez*†

*Theoretical Molecular Biophysics Group, Max Planck Institute of Biophysics, 60437 Frankfurt a.M., Germany

†Cluster of Excellence Macromolecular Complexes, Goethe University Frankfurt, 60437 Frankfurt a.M. Germany

‡These authors contributed equally to this work

METHODS

Classical molecular dynamics simulations

The molecular system in the simulations comprises the complete *Bacillus pseudofirmus* c_{13} rotor, including 46 crystallographic water molecules, 13 of which are in the ion-binding sites; the membrane, with 233 POPC lipids; and ~18,000 water molecules. In total, the system amounts to 99,814 atoms. The rotor ring was inserted into the membrane using the method described by Faraldo-Gómez et al. (1). To equilibrate the model we used a series of molecular dynamics (MD) simulations with gradually weaker structural constraints applied to the protein, over 12 nanoseconds. Subsequent unconstrained simulations extend for 75 nanoseconds. A total of four simulations were performed; one in which E54 is protonated in all subunits of the rotor, and a water molecule is bound to each of the binding sites; and three in which E54 is deprotonated, while a hydronium ion replaces the bound water. Each of these three simulations uses a different parameter set for the classical model of H_3O^+ (see below).

All MD simulations were carried out with NAMD 2.6 (2), using the CHARMM27/CMAP forcefield (3, 4), at a constant temperature of 298 K. Electrostatic interactions were calculated using PME with a real-space cut-off of 12 Å. A cut-off distance of 12 Å was also used for the van-der-Waals interactions. A constant pressure of 1 atm was applied along the membrane normal using a Nose-Hoover Langevin piston; the surface area of the membrane was kept constant, at 69 $Å^2$ per lipid (5).

All three H_3O^+ models considered used atomic charges previously derived from Hartree-Fock 6-31G* calculations and Mulliken population analysis based thereon (6); the models differ in the equilibrium value of the HOH angle, namely 110.4° (6), 106.7° and 113.6° (7). Lennard-Jones parameters were adjusted for each geometry, based on the TIP3P water model, so as to yield a hydration free-energy difference with respect to Na^+ of approx. –7 kcal/mol (8). The modified ε values for oxygen are 0.13613, 0.13993 and 0.13331 kcal/mol, respectively; the corresponding σ/2 values are 1.582539, 1.626744 and 1.547175 Å. The parameters for hydrogen were those in the TIP3P model (ε = 0.046 kcal/mol and σ/2 = 0.2245 Å).

Quantum-mechanical geometry optimizations

Ab initio structure calculations were carried out for a reduced model of the binding site, in the same two states considered in the classical simulations (Fig. 3). These calculations used DFT at the B3LYP/6-31G* level (9-12). In all optimizations the methyl groups capping the truncated model of the binding site were fixed in space. The energy-optimized structures were assessed relative to the crystal structure, as well with respect to each other, using Natural Population and Natural Localized Molecular Orbital analyses (13, 14).

Quantum-mechanical molecular dynamics simulations

Ab initio molecular dynamics simulations of the binding site were carried out to study proton-transfer, using the atom-centered density-matrix propagation method (15-17). In ADMP the electronic structure of the system is represented as a single-particle, electronic-density matrix and is propagated simultaneously along with the classical nuclei, by adjusting the relative nuclear and electronic time-scales. This fictitious dynamics is consistent with Born-Oppenheimer dynamics (18, 19) (BOMD), but is computationally more efficient than BOMD and other extended-Lagrangian methods, e.g. Car-Parrinello (20). This is because the computational cost of ADMP scales linearly with the system size; and also because the larger time-steps make it possible to use an accurate hybrid or gradient-corrected density functional (i.e. B3LYP) as well as chemically accurate basis sets (i.e. 6-31G*).

Based on the crystal structure, and for each of the aforementioned protonation states, we derived slightly different configurations of the binding site as initial conditions for the simulations – these are partial geometry optimizations at the B3LYP/6-31G* level (only of proton coordinates). The subsequent ADMP simulations were carried out in each case for 1 picosecond, using a time-step of 0.25 femtoseconds, at a constant temperature of 298 K (velocity-scaling thermostat). The capping methyl groups were again spatially fixed during the simulations. All *ab initio* calculations were performed with Gaussian 09 (from Frisch M.J. et al., Gaussian Inc., Wallingford CT, 2009).

RESULTS

Quantum-mechanical geometry optimizations

A*b initio* structural optimizations of either configuration of the proton-bound binding site were carried out to assess which one of these configurations most likely corresponds to the experimental structure. It is implicitly assumed that a chemically unrealistic state will result in an optimized geometry that is unlike the crystal structure – while the opposite can be expected for a realistic state.

Indeed, the optimized structure of the model site in which E54 is protonated was found to be in good agreement with the X-ray structure, both in the overall conformation (RMSD ~ 0.5 Å) and coordination distances

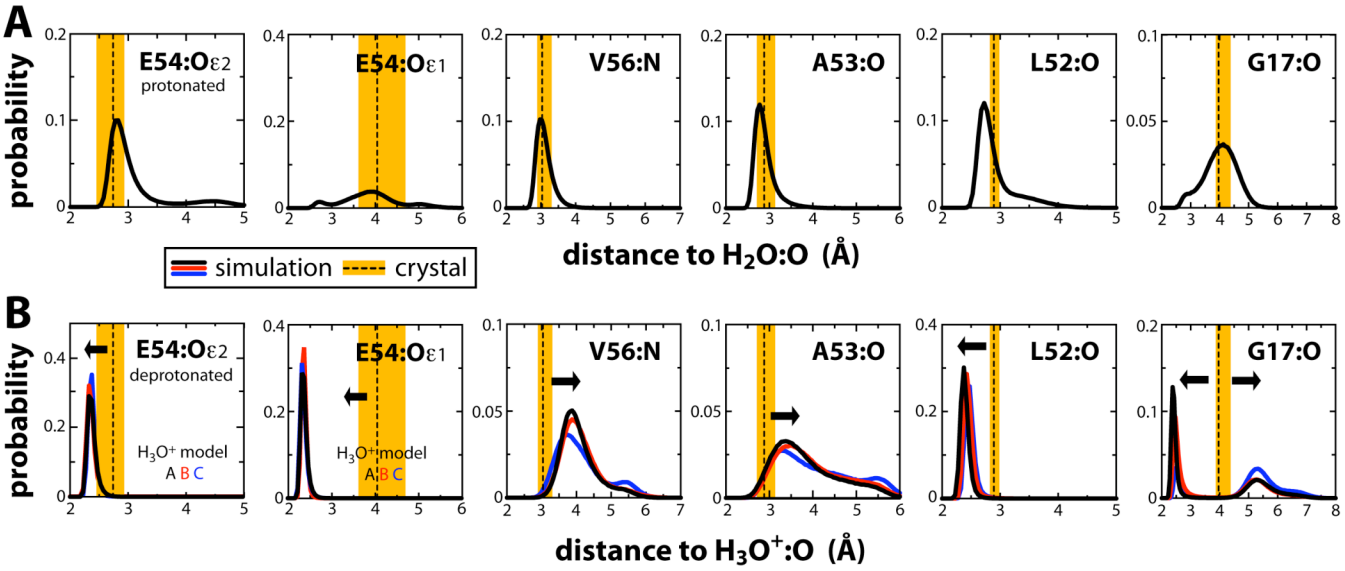

FIGURE S1 Coordination distances in the *Bacillus* c_{13} rotor ring. Average and spread of the crystal-structure values (dashed line, orange band) are compared with calculated ensembles from classical MD simulations of the rotor in a lipid membrane, at ~300 K (solid lines). (A) Simulations in which E54 is protonated, and a water molecule is bound to the binding site; (B) simulations in which H^+ is bound as a H_3O^+ species, and E54 is deprotonated.

(Table 1). Localized molecular-orbital analysis also shows that favorable interactions exist between the lone pairs of carbonyls L52:O and A53:O and the electronic densities corresponding to each of the water hydrogen atoms. The water-oxygen lone pairs also interact favorably with the electron density on the N-H V56 amide dipole, and with that of the protonated E54:Oε2. Summing up, the natural localized molecular-orbital analysis is consistent with an interaction network where E54 is a hydrogen-bond donor, and the bound water molecule is both an acceptor (E54, V56) and a donor (L52, A53). Such a pattern of four hydrogen bonds formed by an individual water molecule is characteristic of deprotonated water clusters (21).

	X-ray structure	Model, H_2O & protonated E54	Model, H_3O^+ & deprotonated E54
V52:O	2.9	2.8	2.6
A53:O	2.9	2.8	5.0
E54:Oε2	2.7	2.7	2.4
E54:Oε1	4.0	4.0	2.4
V56:N	3.0	3.0	3.8

Table S1. Protein-coordination distances (Å) for the bound H_2O / H_3O^+ in the H^+-binding site of the *Bacillus pseudofirmus* c_{13} rotor. The crystal structure is compared with reduced models thereof, after *ab initio* optimizations at the B3LYP/6-31G* level.

The optimizations of the H_3O^+ system are in marked contrast. Incidentally, an additional constraint had to be imposed on the OH bond during these calculations to prevent proton dissociation and subsequent transfer to E54 (the reference OH distance used is from optimized H_3O^+ at the B3LYP/6-31G* level). Even with this additional constraint, the optimizations of the H_3O^+ system did not converge to a well-defined potential-energy minimum, despite negligible forces (< 10^{-6} a.u) and significant structural displacements (~ 0.01 Å). This indicates that the potential-energy surface of the H_3O^+ state is essentially flat. If one among the possible structures on this potential-energy landscape (maximum variability of 0.09 Å) is compared with the carboxylate-protonated configuration, it becomes clear that the H_3O^+ system is highly disfavored, by ~22 kcal/mol.

	H_2O & protonated E54	H_3O^+ & deprotonated E54
V52:O	-0.639	-0.669
A53:O	-0.659	-0.623
E54:Oε2	-0.720	-0.755
E54:Oε1	-0.644	-0.755
V56:N	-0.689	-0.677
V56:H	0.429	0.402
OW	-0.996	-0.889
HW1	0.500	0.526
HW2	0.514	0.532
H*	0.519	0.526

Table S2. Selected atomic charges (a.u.) in the ion-binding site in the *Bacillus* c_{13} rotor, for the two putative configurations of the bound proton (H*). The charges were obtained for geometry-optimized models, using Natural-Population Analysis.

Moreover, although the overall structure of the model-site is not distorted much in the optimization (RMSD ~ 0.7 Å), the coordination distances to the putative H_3O^+ do change noticeably. Localized molecular-orbital analysis shows that these changes reflect the electrostatic repulsion of H_3O^+ with the backbone amide group of Val56, and concurrently, the loss of its hydrogen-bond to A53:O (Table S1). The absence of these interactions is also reflected in the smaller nuclear charge-dipole of the V56 amide, and of the A53 carbonyl, when compared with the

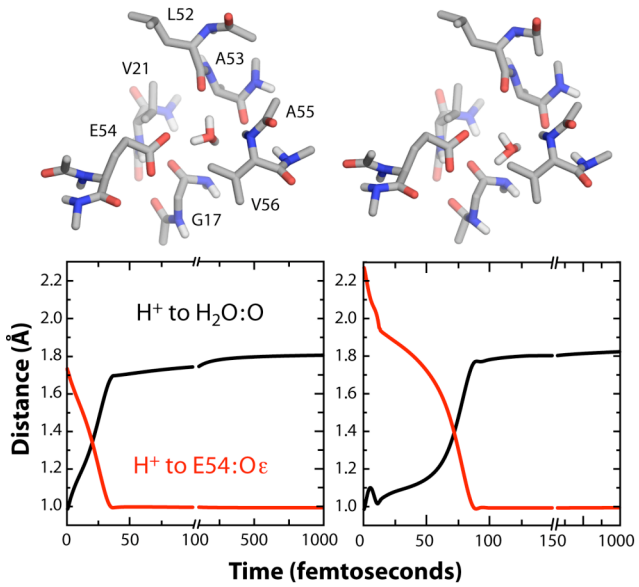

FIGURE S2 ***Ab initio*** **molecular dynamics simulations of a reduced model of the ion-binding site of the** ***Bacillus*** **c_{13} rotor. Two alternative configurations of the putative H_3O^+ state, at the start of the simulations, are shown above the subsequent proton trajectories. Note proton transfer to E54 occurs within 100 femtoseconds in both cases.**

configuration in which E54 is protonated (Table S2). In addition, the V52 carbonyl oxygen becomes more negative as its lone pairs interact at a closer range with the electronic density on the hydronium oxygen. Two other interactions are strengthened, namely between the lone pairs of both E54 carboxylate oxygens, and the electron density from two hydrogen atoms of the H_3O^+ ion; this is consistent with their increased charge polarization (Table S2), and their equivalent hydrogen bond distance (2.4 Å). In conclusion, unlike in the crystal structure, the hydronium ion forms 3 hydrogen bonds with the protein, rather than four, as is expected from previous studies of hydrated H_3O^+ ions (21).

It is worth noting that the classical simulations of the *Bacillus* rotor in the membrane (Fig. 2 and Fig. S1) recapitulate the results from these DFT optimizations point by point. Taken together, these analyses underscore the fact that the crystal structure of the c_{13} rotor (22) does not correspond to the hydronium-bound state, but instead to one in which E54 is protonated and a water molecule contributes to its coordination within the binding site.

REFERENCES

1. Faraldo-Gómez, J. D., G. R. Smith, and M. S. Sansom. 2002. Setting up and optimization of membrane protein simulations. *Eur. Biophys. J.* 31:217-227.
2. Phillips, J. C., R. Braun, W. Wang, J. Gumbart, E. Tajkhorshid, E. Villa, C. Chipot, R. D. Skeel, L. Kale, and K. Schulten. 2005. Scalable molecular dynamics with NAMD. *J. Comput. Chem.* 26:1781-1802.
3. MacKerell, A. D., D. Bashford, M. Bellott, R. L. Dunbrack, J. D. Evanseck, M. J. Field, S. Fischer, J. Gao, H. Guo, S. Ha, et al.. 1998. All-atom empirical potential for molecular modeling and dynamics studies of proteins. *J. Phys. Chem. B* 102:3586-3616.
4. MacKerell, A. D., M. Feig, and C. L. Brooks. 2004. Extending the treatment of backbone energetics in protein force fields: limitations of gas-phase quantum mechanics in reproducing protein conformational distributions in molecular dynamics simulations. *J. Comput. Chem.* 25:1400-1415.
5. Kucerka, N., S. Tristram-Nagle, and J. F. Nagle. 2005. Structure of fully hydrated fluid phase lipid bilayers with monounsaturated chains. *J. Mol. Biol.* 208:193-202.
6. Sagnella, D. E., and G. A. Voth. 1996. Structure and dynamics of hydronium in the ion channel gramicidin A. *Biophys. J.* 70:2043-2051.
7. Hermida-Ramón, J. M., and G. Karlström. 2004. Study of the hydronium ion in water. A combined quantum chemical and statistical mechanical treatment. *J. Mol. Struct. Theochem* 712:167-173.
8. Kelly, C. P., C. J. Cramer, and D. G. Truhlar. 2006. Aqueous solvation free energies of ions and ion-water clusters based on an accurate value for the absolute aqueous solvation free energy of the proton. *J. Phys. Chem. B* 110:16066-16081.
9. Becke, A. D. 1993. Density-functional thermochemistry. III. The role of exact exchange. *J. Chem. Phys.* 98:5648-5652.
10. Lee, C. T., W. T. Yang, and R. G. Parr. 1988. Development of the Colle-Salvetti correlation-energy formula into a functional of the electron-density. *Phys. Rev. B* 37:785-789.
11. Vosko, S. H., L. Wilk, and M. Nusair. 1980. Accurate spin-dependent electron liquid correlation energies for local spin-density calculations: a critical analysis. *Can. J. Phys.* 58:1200-1211.
12. Stephens, P. J., F. J. Devlin, C. F. Chabalowski, and M. J. Frisch. 1994. *Ab initio* calculation of vibrational absorption and circular-dichroism spectra using density-functional force-fields. *J. Phys. Chem.* 98:11623-11627.
13. Reed, A. E., and F. Weinhold. 1985. Natural Localized Molecular-Orbitals. *J. Chem. Phys.* 83:1736-1740.
14. Reed, A. E., R. B. Weinstock, and F. Weinhold. 1985. Natural-Population Analysis. *J. Chem. Phys.* 83:735-746.
15. Schlegel, H. B., J. M. Millam, S. S. Iyengar, G. A. Voth, A. D. Daniels, G. E. Scuseria, and M. J. Frisch. 2001. *Ab initio* molecular dynamics: propagating the density matrix with Gaussian orbitals. *J. Chem. Phys.* 114:9758-9763.
16. Iyengar, S. S., H. B. Schlegel, J. M. Millam, G. A. Voth, G. E. Scuseria, and M. J. Frisch. 2001. *Ab initio* molecular dynamics: propagating the density matrix with Gaussian orbitals. II. Generalizations based on mass-weighting, idempotency, energy conservation and choice of initial conditions. *J. Chem. Phys.* 115:10291-10302.
17. Schlegel, H. B., S. S. Iyengar, X. S. Li, J. M. Millam, G. A. Voth, G. E. Scuseria, and M. J. Frisch. 2002. *Ab initio* molecular dynamics: propagating the density matrix with Gaussian orbitals. III. Comparison with Born-Oppenheimer dynamics. *J. Chem. Phys.* 117:8694-8704.
18. Helgaker, T., E. Uggerud, and H. J. A. Jensen. 1990. Integration of the classical equations of motion on *ab initio* molecular-potential energy surfaces using gradients and Hessians: application to translational energy-release upon fragmentation. *Chem. Phys. Lett.* 173:145-150.
19. Uggerud, E., and T. Helgaker. 1992. Dynamics of the reaction CH_2OH^+ -> $CHO^+ + H_2$: translational energy-release from *ab initio* trajectory calculations. *J. Am. Chem. Soc.* 114:4265-4268.
20. Car, R., and M. Parrinello. 1985. Unified approach for molecular-dynamics and density-functional theory. *Phys. Rev. Lett.* 55:2471-2474.
21. Iyengar, S. S., T. J. F. Day, and G. A. Voth. 2005. On the amphiphilic behavior of the hydrated proton: an *ab initio* molecular dynamics study. *Int. J. Mass. Spectr.* 241:197-204.
22. Preiss, L., Ö. Yildiz, D. B. Hicks, T. A. Krulwich, and T. Meier. 2010. A new type of proton coordination in an F_1F_o-ATP synthase rotor ring. *PLOS Biol.* In press.